The Design of a Radar-Based Navigation System for Large Outdoor Vehicles*

Hugh Durrant-Whyte, Edward Bell and Philip Avery

1 Introduction

This paper describes the design of a navigation system for an Autonomous Guided Vehicle (AGV) system able to transport ISO standard cargo containers in a port environment. The navigation system is based on the use of millimeter wave radar sensors detecting the range and bearing to a number of fixed known beacons. The central navigation algorithm is an extended Kalman filter (EKF) that exploits a model of the vehicle motion and radar observations to continuously provide estimates of the vehicle location.

The use of the EKF to process observations of beacons and to estimate the location of a vehicle is both well understood and widely used in the robotics community [4]. Section 3 provides a brief description of the radars used in the AGV navigation system. Section 4 describes the filter developed for this navigation system. Familiarity with the EKF algorithm is assumed (see [5, 2] for detailed derivations). The main contribution of the system described in this paper lies in the use of a new, and relatively sophisticated, process model describing the motion of a large vehicle, and in the incorporation of this with a novel sensing system. The implementation and validation of the navigation system is described in Section 5. We highlight some of the difficulties in producing a comprehensive validation suite for this type of navigation system.

The vehicle system described here was completed in October 1993 and has since been used in extensive user trials at an operating container terminal in the UK. By way of conclusion, we discuss some of the results of these trials and suggest future research directions essential to commercial exploitation of this type of large outdoor AGV technology.

*The first author is with the Department of Engineering Science, University of Oxford, UK. The second two authors are with Firefly Ltd, UK. This work was conducted in the first authors capacity as technical director of Firefly Ltd.

2 Vehicle Design

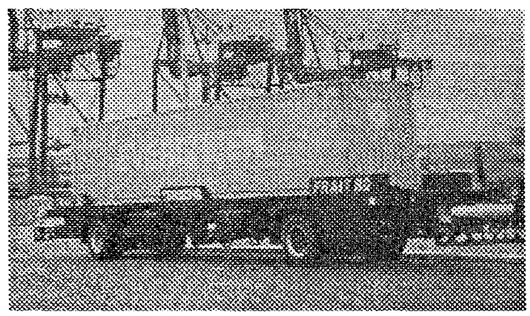

Figure 1: Photograph of Completed AGV with 40 foot Container Load

A photograph of the complete vehicle with load is shown in Figure 1. The vehicle is designed to carry either one ISO 40 foot container (or the planned 50 foot containers), or two ISO 20 foot containers. The vehicle dry weight is 17.5 tonnes. In addition, the vehicle carries 1 tonne of diesel, 0.5 tonnes of hydraulic oil, and a maximum container load of 60 tonnes. The vehicle resembles a conventional trailer in its principle dimensions. The main chassis is 15.5m long, 2.9m wide and 1.6m high. The distance between front and rear axles is 9m, and each of the front and rear bumpers extend approximately 1.3m from the main chassis. Each axle is independently steered. The vehicle drive and steer systems are diesel hydraulic. The hydraulic drive motors are mounted in the wheel hubs. Each steer axle is driven by a pair of conventional hydraulic rams.

IEEE International Conference on Robotics and Automation
0-7803-1965-6/95 $4.00 ©1995 IEEE

3 Navigation Sensors

The vehicle employs two Millimeter Wave Radar (MMWR) units as the primary navigation sensors. These units are mounted at the front and rear of the vehicle below the main cargo deck, at a height of approximately 1.2m from the ground as shown in Figure 1. The radar units are 77GHz Frequency Modulated Continuous Wave (FMCW or chirp) devices [6]. The radars have a swept bandwidth of 600MHz, and sweep time (pulse duration) of 500μs, giving a range resolution of 25cm (which may be improved to 10cm using sub-resolution techniques). The radars have a beam-width of approximately 1^o, and a maximum range of 200m. The beam is mechanically scanned in azimuth at up to 6Hz.

The radar units provide range information from the chirp signal. Bearing information is obtained from encoder measurements of the scanner. The navigation system works by detecting the range and bearing to a set of beacons placed at known, mapped locations about the environment. These beacons are radar trihedrals (effectively internal corner reflectors). The trihedrals return an incident radiation beam directly back along the incident path over the capture angle of the trihedral. Missing or obscured beacons, clutter and false detections are common, but these are dealt with by the navigation algorithm and not through sensor data preprocessing.

4 The Navigation Algorithm

The navigation algorithm is based on the EKF. The algorithm requires that both a **process model** and an **observation model** be defined. Given these models, the EKF provides a simple recursive procedure for computing an estimate of the vehicle location on the basis of predictions made using the process model and measurements made according to the observation model. In the following, familiarity with the details of the EKF and the assumptions necessary for its implementation are assumed.

4.1 The Kinematic Model

The kinematic arrangement of the AGV is shown in Figure 2. The vehicle has a wheel-base of length B. As the wheels on each axle are mechanically

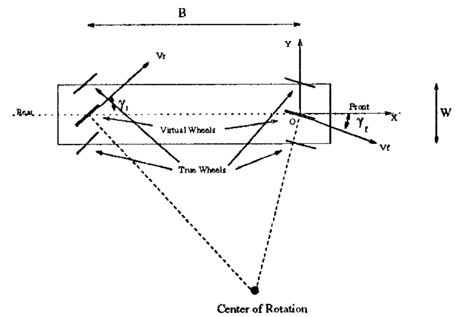

Figure 2: AGV Kinematic Arrangement

linked, it is sufficient (kinematically) to consider each axle as comprising a single central "virtual" wheel, with steer angles γ_f and γ_r, and ground velocities V_f and V_r for the front and rear virtual wheels respectively. The vehicle coordinate system is located at the center of the front axle. Its location and orientation with respect to base coordinates is described by the vector $[x(t), y(t), \phi(t)]^T$. Subject to rolling and rigid body constraints, the equations of motion of this "bicycle" type vehicle are well known [1], and are given by

$$\begin{aligned} \dot{x}(t) &= V_f \cos(\phi + \gamma_f) \\ \dot{y}(t) &= V_f \sin(\phi + \gamma_f) \\ \dot{\phi}(t) &= \frac{(V_f \sin\gamma_f - V_r \sin\gamma_r)}{B}. \end{aligned} \quad (1)$$

4.2 Process Model

The process model is fundamentally important to the correct operation of the navigation filter. The process model described in this section represents a significant improvement on previously published models and is appropriate for vehicles traveling at relatively high speeds on pneumatic tyres over uneven terrain.

We begin with a nominal vehicle model described in continuous time by Equation 1. We make the assumption that the front and rear wheels travel at the same velocity given by the product of an average wheel speed $\omega(t)$ with an average wheel radius $R(t)$ so that $R(t)\omega(t) = V_f(t) = V_r(t)$. Equation 1 then becomes

$$\begin{aligned} \dot{x}(t) &= R(t)\omega(t)\cos(\phi(t) + \gamma_f(t)) \\ \dot{y}(t) &= R(t)\omega(t)\sin(\phi(t) + \gamma_f(t)) \end{aligned}$$

$$\dot{\phi}(t) = \frac{R(t)\omega(t)}{B}\left(\sin\gamma_f(t) - \sin\gamma_r(t)\right)$$
$$\dot{R}(t) = 0, \tag{2}$$

where we have explicitly modeled changes in wheel radius $R(t)$. We now convert Equation 2 in to a discrete-time state transition equation. We assume a synchronous sampling interval ΔT, approximate all derivatives by first-order forward differences, assume all control signals ($\omega(t)$, $\gamma_f(t)$ and $\gamma_r(t)$) are approximately constant over the sample period, and replace all continuous times with a discrete time index as $t = k\Delta T \triangleq k$. Equation 2 then becomes

$$\begin{aligned}
x(k+1) &= x(k) + \Delta T R(k)\omega(k)\cos\left[\phi(k) + \gamma_f(k)\right] \\
y(k+1) &= y(k) + \Delta T R(k)\omega(k)\sin\left[\phi(k) + \gamma_f(k)\right] \\
\phi(k+1) &= \phi(k) + \Delta T\frac{R(k)\omega(k)}{B}\left[\sin\gamma_f(k) - \sin\gamma_r(k)\right] \\
R(k+1) &= R(k).
\end{aligned} \tag{3}$$

The state vector at a time k is then defined as $\mathbf{x}(k) = [x(k), y(k), \phi(k), R(k)]^T$, the control vector as $\mathbf{u}(k) = [\omega(k), \gamma_f(k), \gamma_r(k)]^T$ and the nominal (error-free) state transition as

$$\mathbf{x}(k+1) = \mathbf{f}\left(\mathbf{x}(k), \mathbf{u}(k)\right), \tag{4}$$

where the transition function $\mathbf{f}(\cdot)$ is defined in Equation 3. This defines the nominal process model.

During operation, the true vehicle state $\mathbf{x}(k)$ will never be known. Instead, an estimate of the state is computed through beacon observation and knowledge of the drive signals. Following the notation used in [3], let $\hat{\mathbf{x}}^+(k)$ denote the estimate made of the state $\mathbf{x}(k)$ at time k based on all observations and control knowledge up to time k and let $\overline{\mathbf{u}}(k)$ be the mean measured (from encoders) value of the true control vector $\mathbf{u}(k)$. Following standard practise in the development of the extended Kalman Filter [2], we use Equation 4 to generate a prediction $\hat{\mathbf{x}}^-(k+1)$, of the true state $\mathbf{x}(k+1)$ at time $k+1$ as

$$\hat{\mathbf{x}}^-(k+1) = \mathbf{f}\left(\hat{\mathbf{x}}^+(k), \overline{\mathbf{u}}(k)\right). \tag{5}$$

Errors are injected into the AGV system by three primary sources; forward drive signals, steer angle signals and changes in wheel radius. The forward drive error is modelled as a combination of additive disturbance error $\delta\omega(k)$ and multiplicative slip error $\delta q(k)$

$$\omega(k) = \overline{\omega}(k)\left[1 + \delta q(k)\right] + \delta\omega(k),$$

and the steer error is similarly modelled as a combination of an additive disturbance error $\delta\gamma(k)$ and a multiplicative skid error $\delta s(k)$, assumed to be from an identical source for both front and rear axles

$$\begin{aligned}
\gamma_f(k) &= \overline{\gamma}_f(k)\left[1 + \delta s(k)\right] + \delta\gamma(k), \\
\gamma_r(k) &= \overline{\gamma}_r(k)\left[1 + \delta s(k)\right] + \delta\gamma(k).
\end{aligned}$$

The error in wheel radius is modelled as a discrete additive disturbance rate error (a random walk) so that $R(k) = \hat{R}^+(k) + \Delta T\delta r(k)$. The source errors $\delta q(k)$, $\delta\omega(k)$, $\delta s(k)$, $\delta\gamma(k)$, and $\delta r(k)$ are modeled as constant, zero mean, uncorrelated white sequences, with known constant variances.

The error models for forward drive and steer signals are designed to reflect two important features. First, the multiplicative component of the error models reflect the increased uncertainty in vehicle motion as speed and steer angles increase (slipping and skidding). Second, the additive component of the error models is designed to reflect both stationary uncertainty and motion model errors such as axle offsets. The additive error is also important to stabalize the estimator algorithm. The random walk model for wheel radius is intended to allow adaptation of the estimator to wheel radius changes caused by uneven terrain and by changes in vehicle load (the chassis and wheels deform substantially at loads of 30-60 tonnes).

To develop the error model, we consider how errors in the state estimate and knowledge of control input feed through Equation 3 to generate prediction errors. The error between the true state and estimated state, and between the true state and the prediction are given by $\delta\mathbf{x}^+(k) = \mathbf{x}(k) - \hat{\mathbf{x}}^+(k)$, and $\delta\mathbf{x}^-(k+1) = \mathbf{x}(k+1) - \hat{\mathbf{x}}^-(k+1)$, respectively, the difference between true and measured control input is denoted by $\delta\mathbf{u}(k) = \mathbf{u}(k) - \overline{\mathbf{u}}(k)$, and the error injection source vector is defined as $\delta\mathbf{w}(k) = [\delta\Omega(k), \delta\Gamma(k), \delta r(k)]^T$, where

$$\delta\Omega(k) = \hat{R}^+(k)\overline{\omega}(k)\delta q(k) + \hat{R}^+(k)\delta\omega(k) \tag{6}$$

is the composite longitudinal rate error describing control induced error propagation along the direction of travel, and

$$\delta\Gamma(k) = \hat{R}^+(k)\overline{\omega}(k)(\overline{\gamma}_f(k) - \overline{\gamma}_r(k))\delta s(k) + \hat{R}^+(k)\overline{\omega}(k)\delta\gamma(k) \tag{7}$$

is the composite lateral rate error describing control induced error propagation perpendicular to the direction of travel. Substituting these definitions into Equation 4, linearizing, squaring, and taking expectations with

$$\begin{aligned}
\mathbf{P}^-(k+1) &= \mathrm{E}\left[\delta\mathbf{x}^-(k+1)\delta\mathbf{x}^-(k+1)^T\right], \\
\mathbf{P}^+(k) &= \mathrm{E}\left[\delta\mathbf{x}^+(k)\delta\mathbf{x}^+(k)^T\right], \\
\mathbf{\Sigma}(k) &= \mathrm{E}\left[\delta\mathbf{w}(k)\delta\mathbf{w}(k)^T\right],
\end{aligned}$$

gives an expression for covariance propogation for the filter in the form

$$\mathbf{P}^-(k+1) = \mathbf{F}(k)\mathbf{P}^+(k)\mathbf{F}^T(k) + \Delta T^2\mathbf{G}(k)\mathbf{\Sigma}(k)\mathbf{G}^T(k), \tag{8}$$

where $\mathbf{F}(k)$ is the state error transfer matrix and $\mathbf{G}(k)$ the source error transfer matrix. The transfer matricies are computed as the Jacobians of the state transition model with respect to state and control input.

4.3 Observation Model

After predicting the vehicle location, the next step in the navigation process is to take an observation and to combine this information together with the prediction to produce an updated estimate of the vehicle location. The essential observation information used by the radar consists of measurements of range and bearing made by the radar units to a number of beacons placed at fixed and known locations in the environment.

Processing of observations occurs in four stages. Space precludes the detailed derivation of the equations required for each of these stages.

Stage 1: The radar provides observations of range and bearing to a fixed target in the environment. We assume that the errors in range and bearing may be modeled as an uncorrelated white sequence with constant variance. The range and bearing observations, together with the covariance information is first converted into a cartesian representation referenced to the vehicle coordinate system.

Stage 2: The observation, defined in vehicle coordinates, is now transformed into absolute world coordinates using the predicted vehicle location at the time of observation $\hat{x}^-(k)$. The observation variance is also transformed to base coordinates using the predicted location covariance.

Stage 3: With the observation and observation covariance now in base coordinates, we may now match the measurement with the beacon map. This accomplished using an efficient searching procedure together with a normalized innovation gate [2]. If no beacons are matched, the observation is discarded. If only one beacon is matched, then the update algorithm continues to stage 4. However, if more than one beacon passes the test, then an error is declared. This is to avoid the possibility of generating an incorrect association.

Stage 4: Once a correct association with a single beacon has been made, a vehicle centered observation prediction is generated by transforming the matched beacon from base coordinates back through the predicted vehicle location to the vehicle centered coordinate system. With observation, observation prediction and predicted vehicle location, together with all covariance information, the updated vehicle estimate may now be computed from the usual Kalman filter equations.

5 Implementation

5.1 Architecture

The navigation system runs on a system comprising two DSPs and two Transputers. The DSPs are dedicated to preprocessing of radar signals and indeed are physically located in the radar housings. The two Transputers run the main navigation code. The navigation system is part of a much larger system incorporating control, safety, condition monitoring and planning systems, but here it is treated as much as possible as a "black-box". The cycle rate for the filter is 20Hz. The the state prediction component of the navigation filter, running on the first Transputer, generates synchronous predictions of vehicle location and its associated covariance every 50ms. The prediction is based on synchronous measurements of drive and steer signals together together with the previous state prediction. Observation information is processed on the second Transputer which reads in data from the radars asynchronously. Prediction information from the first Transputer is used to generate an estimated vehicle location at the observation time. This is used to transform the observation to base coordinates, generate a match with the beacon map and translate this back in to vehicle centered coordinates. Successful matches are passed back to the first Transputer to be used for updating.

5.2 Validation Process

The validation of this type of navigation system is surprisingly difficult. This is for two main reasons.

1. It is impossible to know exactly what the "true" location of the AGV is at any given time, and so it is difficult to find any absolute measure of how well the navigation system is performing.
2. Standard residual-type measures of performance are difficult to use as the measurement process depends heavily on which beacon is being observed.

To overcome these problems, the validation of the navigation system and software was accomplished in 3 phases.

1. Independently calibrated trials of the radar units were performed. The radars were placed on a buggy on a 200m long railway line, calibrated for absoulte distance to 5mm. A number of different beacon layouts were tested at all ranges. Calibration curves were produced together with detection and gating probabilities.
2. The radars were placed on the vehicle. The vehicle was equipped with a paint drip and required to move up and down in a straight line of about 200m. The paint tracks were then surveyed in to the beacon map. This provided a coarse absolute measure of straight-line accuracy. Repeat tests with container clutter were performed. Tests on curved tracks proved to be impossible to check absolutely.
3. Repeatability tests were performed in which the vehicle was required to execute a path, comming to a halt at specific places where location and orientation were measured. A typical trial involved the vehicle executing the same trajectory continuously for periods of about 12 hours.

The validation process was undertaken over a six-month period. It highlighted some major problems in the generation of absolute performance measures for this type of AGV system. Ideally, what is needed is an independent measure of vehicle position that can be compared to those estimates generated by the vehicle navigation system. In practise, no such measure is possible as no other sensor can operate in the same conditions and to the same accuracy as the radar (and indeed if there were such a sensor, it would be used as the navigation sensor instead of the radar !).

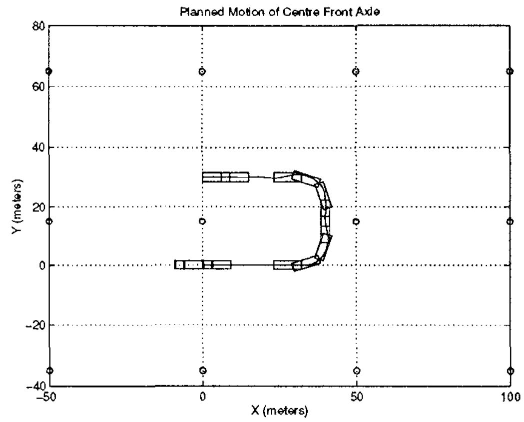

Figure 3: A Typical Executed Path

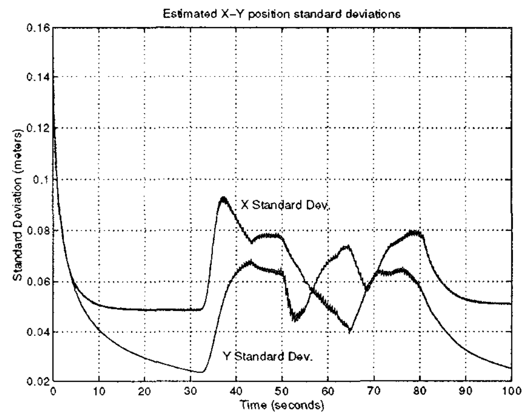

Figure 4: Standard Deviation of x and y position estimates

From a stationary position, the vehicle accelerates to 4m/s. A 90^o turn is then executed and the vehicle continues along at constant speed. A second 90^o turn is then executed and then the vehicle decelerates to a stop. The path length is approximately 200m. As described, analysis of 'true' vs estimated vehicle location is not possible, however, estimated standard deviations do provide some measure of performance. For the path shown in Figure 3, estimated standard deviations increase from approximately 2cm when the vehicle is static, to a maximum of 6cm during turning, with a steady level of approximately 4cm on a straight path Figure 4. Estimated standard deviation depends heavily on the density and layout of beacons in the area. Space precludes the prentation of detailed results.

5.3 Application Trials

The vehicle system described in this paper was installed at an operating container port on the southern coast of England. Installation took place over a 6 month period and was completed in October 1993. We briefly describe here some of the main points of the installation and the main problems experienced during operations so far.

The installation area consisted of a main stacking and quay area. The total installation area is approximately 2 square kilometers, with a quay length of about 600m. Typical cycles from yard to ship are about 1-2Km. A total of 150 beacons were set up to cover the operation area. In the yard area, these were placed along roadways between container stacks at intervals of approximately 40m. Elsewhere, the beacons were placed so as to tessellate the ground area with a triangle grid of base dimension 50m (this maximizes location accuracy).

The most immediate problem faced was the very high level of clutter experienced by the radar in a container environment. A great deal of time was spent adjusting radar sensitivity and improving gating procedures to overcome this problem. Major changes in reflectivity of the environment caused by rain and snow also caused sever problems. Some of these were overcome by employing probabilistic gating and association algorithms. The use of very tight gating procedures, at the expense of low matching rates, substantially improved system reliability.

A second important problem was the detection of navigation faults due to mis-matching and drifting of system components and estimates. The difference in estimates pre and post update were used to identify abrupt faults due to mismatching and sudden load changes. However, low frequency drifts in component values (radar calibration, steer slippage, geometry change with temperature, etc), proved very difficult to isolate. Augmented estimators were developed to accommodate this type of condition and to monitor changes in slowly varying parameters. These worked well enough to overcome immediate problems.

Some anticipated problems turned out to be much less important than expected. In particular, the navigation system processing was rarely a source of system failures (this tended to be dominated by faults in other vehicle components such as hydraulic system sensors, controllers, etc). The loss of beacons through obscuration or from deliberate vandalism (by dockers) was also not a problem, and rarely resulted in navigation performance below specification.

6 Conclusions

The AGV system described in this paper represents an important step in the commercialization of advanced mobile robot ideas. The system exploits what is seen as the "state of the art" in sensing and navigation technology. The development of the AGV has highlighted a number of important issues that will need to be addressed by the robotics community as techniques developed in the laboratory mature to become commercial systems. In particular, the need to develop and build reliability in the context of autonomous systems is seen as crucial. This requires a careful re-think of the way in which techniques and systems are developed, and the further development of quantifiable measures of performance and reliability at both component and system levels.

[1] J.C. Alexander and J.H. Maddocks. On the kinematics of wheeled mobile robots. *Int. J. Robotics Research*, 8(5):15-27, 1989.

[2] Y. Bar-Shalom and T.E. Fortmann. *Tracking and Data Association.* Academic Press, 1988.

[3] M. Gelb. *Applied Optimal Estimation.* MIT press, 1974.

[4] J.J. Leonard and H.F. Durrant-Whyte. *Directed Sonar Navigation.* Kluwer Academic Press, 1992.

[5] P.S. Maybeck. *Stochastic Models, Estimaton and Control, Vol. I.* Academic Press, 1979.

[6] M.I. Skolnik. *Introduction to Radar Systems.* McGraw-Hill, 1980.